Dispersive charge transport along the surface of an insulating layer observed by electrostatic force microscopy

Jérôme Lambert,* Grégoire de Loubens, Claudine Guthmann, and Michel Saint-Jean
Groupe de Physique des Solides, Campus Boucicaut, 140 rue de Lourmel, 75015 Paris, France

Thierry Mélin
Institut d'Electronique de Microélectronique et de Nanotechnologie—CNRS UMR 8520–Avenue Poincaré, BP 69, 59652 Villeneuve d'Ascq Cedex, France

(Received 9 August 2004; published 26 April 2005)

We report the observation in the direct space of the transport of a few thousand charges submitted to a tunable electric field along the surface of a silicon oxide layer. Charges are both deposited and observed using the same electrostatic force microscope. During the time range accessible to our measurements (i.e., $t=1-1000$ s), the transport of electrons is mediated by traps in the oxide. We measure the mobility of electrons in the "surface" states of the silicon oxide layer and show the dispersive nature of their motion. It is also demonstrated that the saturation of deep oxide traps strongly enhances the transport of electrons in the surface plane, in the direction of the electric field.

DOI: 10.1103/PhysRevB.71.155418 PACS number(s): 72.80.Sk, 72.20.−i, 68.37.Ps

I. INTRODUCTION

The development of Electrostatic Force Microscopies allows now to measure precisely the electric characteristics of surfaces. For instance, measurements of contact potential,[1–3] polarization charges,[4] embedded charges or deposited charges on insulating surfaces[5–7] or quantum dots[8,9] have been performed. The relaxation of excited charges may also be studied by EFM: the charges can be photo-excited,[10] or deposited charges (either on oxides surfaces[11] or on nanocrystals [8,9]). Recently, charge transport in arrays of nanocrystals has been observed.[12]

We describe here an original experiment performed in order to discuss the transport mechanism involved in the motion of the charges on amorphous dielectric surfaces. Using an Electrostatic Force Microscope, a charge packet is deposited on a SiO_2 surface between two embedded electrodes. These latter induce a "transverse" electric field along the insulating surface. The temporal evolution of the charge packet on such a layer is scanned in the direct space with the same EFM. This experiment is schematized in Fig. 1.

In this kind of amorphous oxide, the nanoscopic transport mechanism is electronic hopping between traps, the origin of which is due either to impurities embedded in the bulk—deep traps—or to the disorder—shallow traps. From the theoretical point of view, one may distinguish two "limit" cases, the diffusive and dispersive transports, that lead to qualitatively different behaviors of a charge distribution submitted to an electric field. In the case of classical diffusive transport, the mean displacement of a charge packet can be described by a mobility and its spreading remains symmetric.[13,14] On the other hand, in the case of dispersive transport, the position of the maximum of the charge distribution is no longer the same as the position of its mean since its evolution is then dissymmetric.[13,14] Thus, the observation of a charge packet motion under a constant electric field represents a fundamental challenge in order to characterize the transport. However, the experiments usually performed to study these phenomena involve macroscopic measurements of transient currents across the insulators and do not allow a precise determination of their spatial characteristics. Indeed, these measurements integrate the contributions of the whole charge distribution over the thickness of the insulating layer[13,15–17] and thus the characterization of the spatial distribution of charges in the insulating layer from the current measurements requires *ad-hoc* assumptions.

By contrast, since the EFM allows to work at the mesoscopic scale, our experiments enable to obtain directly this spatial charge distribution and then allow a better understanding of the transport.

Our observations show that a charge distribution deposited on a SiO_2 surface is mobile under the influence of an electric field comparable to those obtained in a normal electronic device such as a MOSFET: One may clearly observe a spatial dissymmetrization of the charge distribution, sometimes accompanied by an observable shift of the maximum of the charge distribution. In addition, we show that this motion is strongly influenced by the fact that the insulating surface has previously been charged or not.

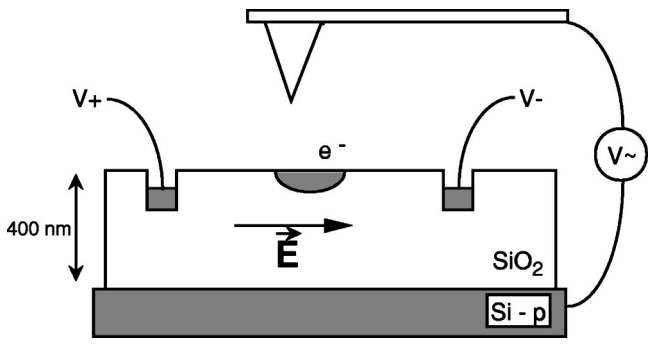

FIG. 1. Schematic diagram of the device and of the experimental set-up.

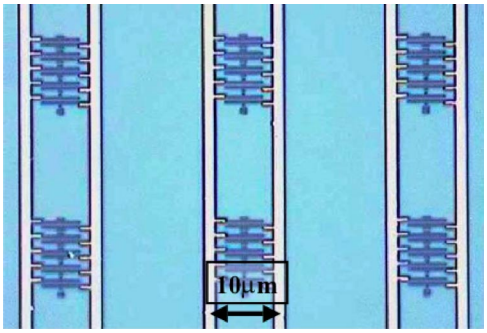

FIG. 2. (Color online) Optical microscopy view of interdigitated electrodes embedded in a 400 nm thick SiO_2 layer.

II. EXPERIMENTAL SETUP

We selected thermal silicon dioxide as the insulating material in order to elaborate the device adapted to our experiments. The obtention of the transverse electric field at the surface of the layer is achieved by embedding interdigitated electrodes in the bulk during its elaboration.

We chose this oxide mainly for its technological interest; in addition, its integration in microelectronic devices has induced the mastering of its homogeneity, an essential requirement in our experiment. Moreover, the samples offer the possibility to incorporate electrodes and contacts at any stage of their making. This latter point was crucial since the electrodes had to be buried in the insulator in order to minimize their electric influence on the EFM tip and to ensure a maximum transverse field within the insulating layer.

Our experiments were performed using devices prepared from a 400 nm thick thermal silicon dioxide layer grown on a *p*-type doped silicon wafer. Interdigitated electrodes arrays with electrodes spacing of 10 μm (depth 60 nm) were made by electron-beam lithography. The transfer of the polymethylmetacrylate mask into the silicon dioxide layer is achieved by wet etching with a dilute hydrofluric acid solution and followed by a 25 nm thick titanium metallization. The lift-off is performed in aceton and followed by a rinsing step in propanol and deionionized water). Figure 2 shows the optical image of a typical device. Each array includes five pairs of electrodes. The distance between two electrodes of the same pair is 1 μm. Two neighbor pairs are 3 μm distant. Thus three characteristic distances are available in this setup: 1, 3 and 10 μm. This allows us to tune the electric field induced by these electrodes.

In order to deposit and to measure charges of both signs on the SiO_2 surface, we developed a homemade modified electrostatic force microscope (EFM). An important advantage of this EFM is to allow both charge injection and measurements experiments with the same apparatus. A complete description of the different operating modes of this instrument can be found in Félidj *et al.*[11] Let us be reminded here of its main characteristics. All our experiments are performed in a vacuum chamber first outgassed during 24 H, then filled with dry nitrogen gas in order to avoid any water pollution on the surface of the insulating layer.[7]

According to the seminal procedure proposed by Stern *et al.*,[5] the charges are deposited by contact electrification. During the deposition procedure, an EFM Pt-coated tip, fixed on a cantilever, is slowly brought in contact with the SiO_2 layer. During this down motion, the potential V_0 of the tip is kept equal to 0 V. Once the contact is achieved, the tip stays at the same contact point while a voltage V_d ($-100\ \mathrm{V} < V_d < +100\ \mathrm{V}$) is applied during the contact time $t_d = 1$ ms between the tip and the conductive substrate of the insulating layer. The quantity of deposited charges varies linearly with V_d. Moreover their spatial distribution can be chosen by tuning the deposit voltage and the deposit time.[18] Once the deposit is achieved, the tip is withdrawn from the surface. Right after this withdrawal, the tip starts scanning the charged surface. The tip-surface distance is kept constant ($z \approx 20$ nm) in order to select the electrostatic force as the dominant force contribution[19] and to minimize the perturbations induced by the tip on the deposited charges.

We use the EFM in the resonant mode. In this operating mode, the cantilever is excited by a bimorph near its resonance frequency ω (about 100 kHz) and the tip oscillates at an amplitude of a few angströms. In addition, a modulated voltage $V_0 + V_1 \sin(\Omega t)$ (Ω about 10 kHz), is applied between the tip and the conductive substrate of the insulating layer. The resulting force exerted on the tip results from this potential and from the potential V_σ induced by the deposited charges (only electrostatic forces are taken into account for tip surface distances larger than 10 nm). This force is then a sum of three components oscillating at frequencies ω, Ω and 2Ω respectively:

$$F_\omega = \frac{\partial_z C(z)}{2}\left[(V_0 + V_\sigma)^2 + \frac{V_\Omega^2}{2}\right],$$

$$F_\Omega = \partial_z C(z) V_\Omega (V_0 + V_\sigma), \tag{1}$$

$$F_{2\Omega} = \frac{\partial_z C(z) V_\Omega^2}{4},$$

where $C(z)$ is the tip-surface capacitance and z is the tip-surface distance. The vibration amplitude of the cantilever is strongly modified when forces are exerted on the tip. These amplitudes and their variations are measured, by interferometric methods, above each point of the scanned surface. By analyzing them using synchronous detections it is possible to obtain the different contributions to the force at frequencies Ω, 2Ω, ω and to determine the spatial characteristics of the charge distribution from F_Ω. A feedback loop keeps the value of A_ω (proportional to dF_ω/dz) constant during the scan; then one may measure simultaneously the variations of z and F_Ω.

As an illustration, Figs. 3(a) and 3(b) show, respectively, topographical and electrical images of a polarized electrode recorded simultanously. One may read separately both electrical and topographical information. In this configuration, the field induced at the surface of the silicon dioxide layer is approximately $10^4\ \mathrm{V\ m^{-1}}$. This is a weak value compared to those suggested by the dimensions of the electrodes and by the lateral bias; this is due to the fact that the conducting doped silicon substrate (counter-electrode) screens the field induced by the embedded electrodes. Hereafter this electric field will be designated as a "transverse" electric field in

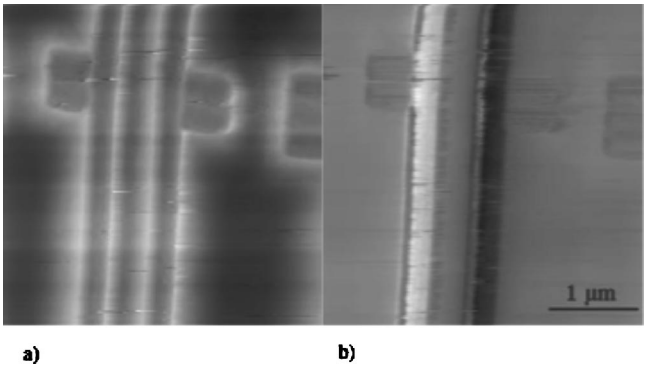

FIG. 3. EFM images of biased electrodes: (a) topographical signal; (b) electrical signal. The two electrodes are put, respectively, at biases +2.85 V (left) and −2.85 V (right).

contrast with the field induced by the tip in the insulating layer. Between these electrodes, the EFM charge deposits were found similar for all samples, their characteristic size being about 500 nm wide.[7,20]

III. EXPERIMENTAL RESULTS

Before describing the influence of a transverse electric field on a charge packet, let us first describe the typical relaxation of such a packet when no external electric field is exerted. This behavior is characteristic of the oxide since similar results have been obtained on samples with or without electrodes. These results are in perfect agreement with those we previously obtained on high-K oxides.[11] For instance, let us consider a positive charge packet deposited by contact electrification (V_d=−40 V) on the uncharged dioxide surface of the array, the embedded electrodes being unpolarized. The evolution of the recorded profile of this charge distribution is pictured in Fig. 4(a) (the recording starts 1 s after the charge deposit). The dimensions of this distribution are considerably larger than the radius of the apex of the EFM tip: therefore one may consider that the charge distribution can be described by a surface charge density.[20] The force exerted on the tip is then strictly proportional to this charge density under the tip integrated over the whole thickness of the layer.[11,15] One may thus evaluate the total charge quantity which has been deposited (a few thousand charges). By comparing the normalized charge profile measured at different steps of its evolution [Fig. 4(b)] we can observe the absence of profile drift and of spreading of the charge distribution during its relaxation. These behaviors can simply be interpreted if we consider the fact that the charges move by hopping in such insulating materials. During the contact, the electric field induced by the tip in the insulating layer possesses both large parallel ("transverse") and perpendicular to the surface components:[21,22] The injected charges instantaneously wet the oxide surface by filling the electronic states located near the surface. In this frame, the large extension (about 500 nm) of the initial deposit is due to the transverse electric field which assists the hopping along the surface. When the tip is raised, this transverse component resulting from the tip curvature disappears and no more spreading

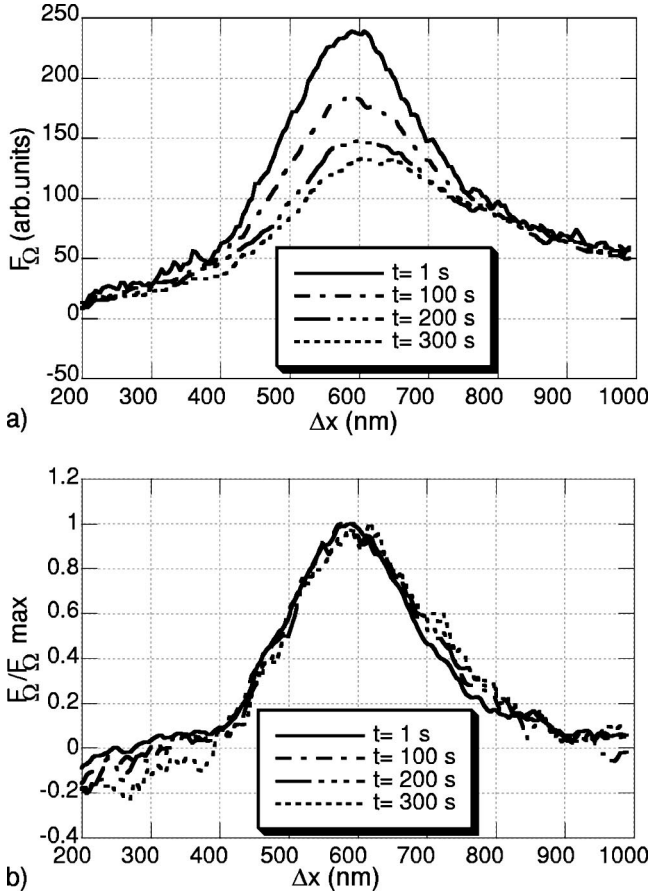

FIG. 4. (a) Electrical profiles recorded above a charge distribution, resp., 1, 100, 200, and 300 s after the deposit. The deposit was performed at V_d=−40 V. The total width is 1 μm. (b) The same profiles after normalization by their respective maximum values.

along the surface can be observed. By contrast, in these experimental conditions, the electric field resulting from the interaction between the deposited charges and their images in the conductive substrate is important and results in a transport process across the layer, which is the dominant mechanism for the diffusion of the charge packet. On the other hand, from the instrumental point of view, these results provide important information concerning our experiments: they show without ambiguity that our experimental setup does not induce any drift due, for instance, to the piezoelectric ceramic relaxation.

Two different types of behavior of the deposited charges are observed under a transverse electric field, depending on whether the insulating layer had previously been charged or not. Let us first consider the evolution, under the influence of an applied transverse electric field, of a charge packet deposited on a surface upon which no deposit has previously been performed. The charges are deposited between the electrodes, around 5 μm far from them. At this distance, the effect of the image charges in the electrode is negligible. We chose this configuration in order to obtain a homogenous transverse electric field on the whole spreading of the charge packet.

Figure 5 shows the evolution of the electric force profile with time in such a situation. One may see a very slight

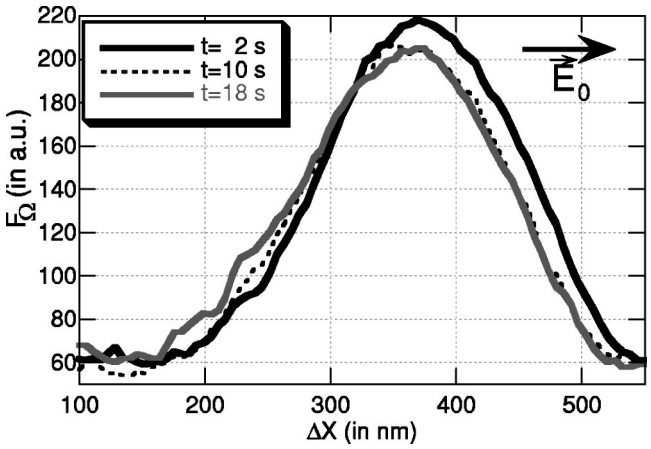

FIG. 5. Temporal evolution of $F(\Omega)$ above a 1.5 μm segment of the SiO_2 surface centered on a charge deposit performed with $V_d = +50$ V, $t_d = 200$ ms. The electric field is oriented in the direction of the arrow.

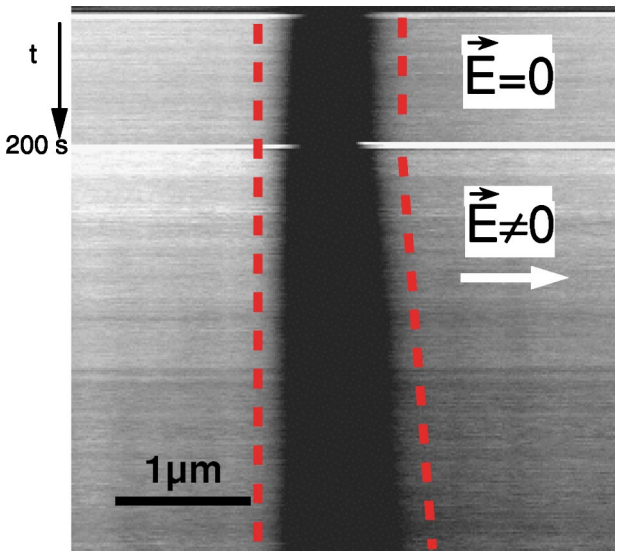

FIG. 6. (Color online) Top view: time evolution of F_Ω on a SiO_2 surface. Each line corresponds to a recording of the force as the tip passes over the deposited charge. $V_d = -100$ V. At $t = 200$ s, the transverse electric field is turned on. Its orientation is indicated by the white arrow.

deformation of the charge packet soon after the deposit, which is stopped typically after a few tens of seconds. No drift of the topography is observed. The small drift of the charges is outlined by the crossing of successive profiles on one side of the charge distribution, whereas the position of the maximum of the charge distribution, corresponding to the maximum of the force exerted on the tip, seems to be constant. This slight displacement is parallel to the electric field and in the left direction with respect to the sign of the charges. Let us emphasize that this behavior is characteristic and was obtained for several deposits, for charges of both signs.

In order to highlight this small movement of the charges, we performed experiments in which we focused on the evolution of the feet of the charge distribution. In these experiments, the charge are first left to diffuse without any applied transverse electric field during 200 s. During this stage, the charges penetrate inside the oxide: thus the feet of the both sides of the distribution are not shifted in the top view representation of the charge profile presented in Fig. 6. The profile width is constant, in agreement with the behavior discussed before. In contrast, as soon as the transverse electric field is turned on, 200 s after the deposit, an asymmetric diffusion can be observed on the top view profiles: one side of the charge distribution moves slightly whereas the other one is unchanged.

These two experiments lead us to emphasize the fact that only a small fraction of the deposited charges really move significantly under the transverse electric field and that this fraction diminishes as the relaxation across the layer goes on. Qualitatively, we suggest that mobile charges progressing in a surface never charged before discover empty deep traps and are progressively trapped by them.

The experiments described above suggest that the mobility of the carriers would be larger if the deep traps were not available to trap them. In order to test this assumption and to maximize the number of charges involved in the transverse displacement of the packet, we performed specific experiments in which we initially fill the traps with charges originating from a first deposit. Thus, a first packet of a few thousands positive charges is deposited by applying a voltage $V_d = -60$ V on the tip during 1500 ms. The full width at half maximum of this charge distribution is about 500 nm: in agreement with our previous comment, this large extension suggests that the injected charges wet the surface very far from the injection point of contact. In order to ensure that the free charges fill the most accessible deep traps, this packet is left to diffuse during 100 s without any applied transverse electric field. After this delay, a second charge deposit is performed in the same conditions near the first charge packet. The distance between the two deposits is approximately 1 μm. As soon as this second packet is deposited, the transverse electric field is turned on. The maximum of the first charge distribution does not move and only a small distortion of the packet under the force exerted by the electric field can be observed. This behavior is similar to those previously discussed in the case of a single charge deposit submitted to a transverse electric field. This confirms our initial assumption according to which, 100 s after the deposit, only a small fraction of the charges are not trapped in deep traps and can thus be moved. The main feature is indeed the evolution with time of the second charge packet. Figure 7 pictures this evolution: one observes an important drift of the maximum and a strong distortion of the distribution. This indicates that a large fraction of the charges belonging to this packet move now under the influence of the transverse electric field, amplifying its lateral displacement. As expected, the charges of the second deposit are more mobile than the charges belonging to the first deposit. In order to characterize more precisely the mobile charge transport from our measurements, we computed the time evolution of the displacement of the maxima of the charge packets together with the first momentum of the single-variable distribution extracted from the measurements of the profiles—This procedure

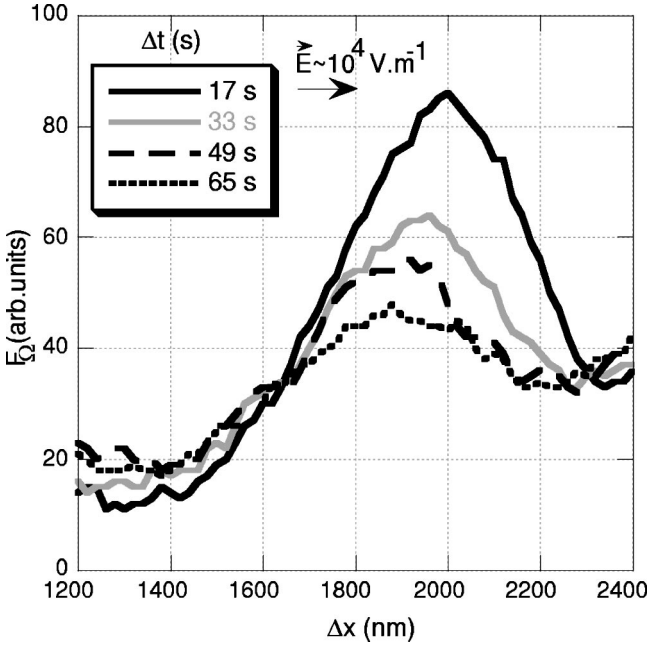

FIG. 7. Four recordings of the force exerted on the tip as it passes above a charge distribution submitted to a transverse electric field ($E \approx 10^4$ V m^{-1}). Recording times are, respectively, 17, 33, 49, 65 s after the deposit.

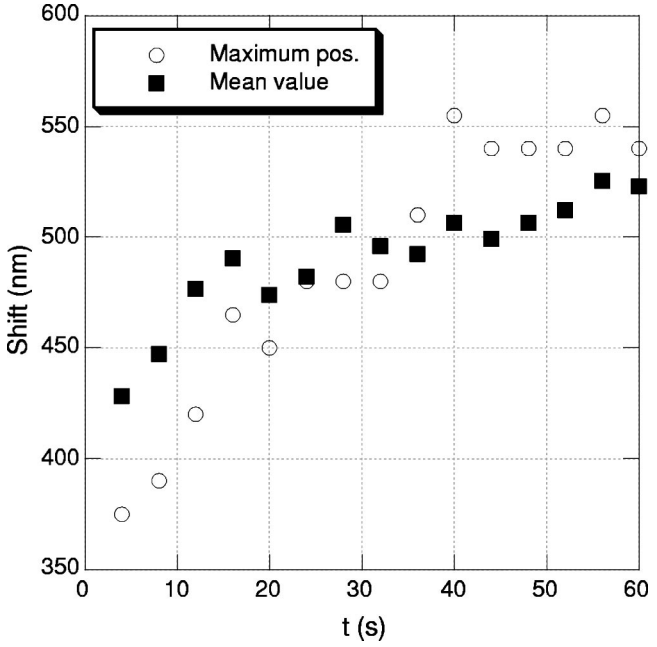

FIG. 8. Time evolution of the shift of the maximum and of the mean value $\langle x \rangle$ of the charge distribution pictured in Fig. 7. A linear fit of $\langle x \rangle$ gives a value for the mobility of the charge distribution.

might seem risky since the total number of charges involved in the transverse transport may not be considered as constant because of the disappearing of some charges in the counterelectrode—their behaviors being similar or not according to the transport mechanisms involved. For instance, in the canonical case of diffusive transport, the evolution of the maximum and of the mean of the charge distribution deduced from the profiles should be parallel. Figure 8 shows the time evolution of both quantities. The maximum of the packet has not the same behavior as its mean position, thus suggesting a dispersive transport. In a first approximation, we suppose that the transverse and in-depth transport are decoupled, and thus that the fraction of charges involved in the transverse transport is constant at any time, even if the total number of these charges decreases with time. This hypothesis is reinforced by the experimental evidence that the free charge distribution previously described does not spread, although the transverse electric field is by no means homogeneous as one goes from the middle to the borders of the distribution: the charges seem to drift towards the counterelectrode at the same speed regardless of the transverse electric field to which they are submitted. Fitting linearly the evolution of the first momentum gives an estimation of the mobility of the charges under the transverse electric field: $\mu = 0.15$ cm^2 s^{-1} V^{-1}; a value which is less by two orders of magnitude than the one usually reported for electrons in the conduction band in SiO_2 (e.g., Mott gives $\mu_e = 20$ cm^2 s^{-1} V^{-1} in Ref. 23), but which is much larger than the value of the mobility reported for holes in the same material ($\mu_h = 10^{-6}$ cm^2 s^{-1} V^{-1}). This result is compatible with our assumption after which the moving charges are electrons hopping from trap states to trap states below the conduction band.

IV. CONCLUSION

To conclude, let us recall the main experimental results presented in this Letter: With no applied transverse electric field, the charges deposited on the silicon oxide surface are attracted by their images in the counterelectrode and move inside the layer. We show in particular that no spreading of the charge packet is observed. During this migration, there is no diffusion along the surface. A very different behavior can be observed when a transverse field is applied between the two embedded electrodes. In this case, the deformation of the deposited charge packet is clearly identified and measured. Its amplitude depends on the state of charge of the insulating surface: the drift is larger in the case of initially charged surfaces. This result indicates that the lateral displacement is mediated by the electric field through the traps located in the oxide surface (over a width of a few tens of nm) in the oxide and that the dynamic characteristics of the charge packet are controlled by the trapping-escaping processes of the electrons. Moreover, with this experiment, we can answer the important question of the nature of the transport in such systems. We restricted ourselves to a qualitative estimation of the transport by noticing the strong spreading and loss of symmetry of the second charge distribution, indicating that the transport is not diffusive, if not completely dispersive. A more precise description of the transport would require the computation of the following momenta of the distribution in order to characterize precisely the spreading, the loss of symmetry and the flattening of the charge distribution (For example, in the case of dispersive transport, Scher and Montroll found that the time evolution of the first and second momenta were alike.)

Hence, this observation of the displacement of deposited charges along insulating surfaces in the direct space allows

us to discuss more precisely, and without ambiguity, the behavior of electrons in insulator surfaces containing traps; hence we believe this kind of analysis is promising in both fundamental and technological areas. Let us notice that a more quantitative analysis of the behavior of the charges should be led very carefully, since rare events-driven systems of small sizes may exhibit a wide variety of behaviors.[24] This dispersion of behaviors might, in itself, provide interesting informations about the characteristic lengths involved in this type of transport.

ACKNOWLEDGMENTS

The authors acknowledge C. Boyaval for the elaboration of the devices and F. Breton for his outstanding technical assistance.

*Electronic address: jerome.lambert@univ-rennes1.fr; now at GMCM, Université Rennes1—UMR 6626, Bâtiment 11A—Campus Beaulieu, 35042 Rennes cedex, France.

[1] M. Nonnenmacher, M. P. O'Boyle, and H. K. Wickramasinghe, Appl. Phys. Lett. **58**, 2921 (1990).

[2] N. Nakagiri, T. Yamamoto, H. Sugimura, and Y. Suzuki, J. Vac. Sci. Technol. B **14**, 887 (1996); URL http://link.aip.org/link/?JVB/14/887/1

[3] K. Domanský, Y. Leng, C. C. Williams, J. Janata, and D. Petelenz, Appl. Phys. Lett. **63**, 1513 (1993); URL http://link.aip.org/link/?APL/63/1513/1

[4] J. Lambert, C. Guthmann, C. Ortega, and M. Saint-Jean, J. Appl. Phys. **91**, 9161 (2002).

[5] J. Stern, B. Terris, H. Mamin, and D. Rugar, Appl. Phys. Lett. **53**, 2717 (1988).

[6] C. Schönenberger, Phys. Rev. B **45**, 3861 (1992).

[7] M. Saint-Jean, S. Hudlet, C. Guthmann, and J. Berger, Eur. Phys. J. B **12**, 471 (1999).

[8] E. Boer, M. Brongersma, H. Atwater, R. Flagan, and L. Bell, Appl. Phys. Lett. **79**, 791 (2001).

[9] T. Mélin, H. Diesinger, D. Deresmes, and D. Stievenard, Phys. Rev. B **69**, 035321 (2004); URL http://link.aps.org/abstract/PRB/v69/e035321

[10] C. C. Williams, J. Slinkman, W. P. Hough, and H. K. Wickramasinghe, J. Vac. Sci. Technol. A **8**, 895 (1990); URL http://link.aip.org/link/?JVA/8/895/1

[11] N. Félidj, J. Lambert, M. Saint-Jean, and C. Guthmann, Eur. Phys. J.: Appl. Phys. **12**, 85 (2000).

[12] M. Drndić, R. Markov, M. V. Jarosz, M. G. Bawendi, M. A. Kastner, N. Markovic, and M. Tinkham, Appl. Phys. Lett. **83**, 4008 (2003); URL http://link.aip.org/link/?APL/83/4008/1

[13] R. Zallen, *The Physics of Amorphous Solids* (Wiley, New York, 1983).

[14] H. Scher and E. Montroll, Phys. Rev. B **12**, 2455 (1975).

[15] I. Batra, K. K. Kanazawa, B. Schechtman, and H. Seki, J. Appl. Phys. **42**, 1124 (1971).

[16] H. Wintle, J. Appl. Phys. **43**, 2927 (1972).

[17] K. K. Kanazawa, I. Batra, and H. Wintle, J. Appl. Phys. **43**, 719 (1972).

[18] M. Saint-Jean, S. Hudlet, C. Guthmann, and J. Berger, Phys. Rev. B **56**, 15 391 (1997).

[19] M. Saint-Jean, S. Hudlet, C. Guthmann, and J. Berger, J. Appl. Phys. **86**, 5245 (1999).

[20] J. Lambert, C. Guthmann, and M. Saint-Jean, J. Appl. Phys. **93**, 5369 (2003).

[21] J. Lambert, M. Saint-Jean, and C. Guthmann, J. Appl. Phys. **96**, 7361 (2004).

[22] T. Gross, C. Prindle, K. Chamberlin, N. bin Kamsah, and Y. Wu, Ultramicroscopy **87**, 147 (2000).

[23] N. F. Mott, *Conduction in Non-Crystalline Materials* (Clarendon, Oxford, 1987).

[24] V. D. Costa, Y. Henry, F. Bardou, M. Romeo, and K. Ounadjela, Eur. Phys. J. B **13**, 297 (2000).